Activation of the P2RX7/IL-18 pathway in immune cells attenuates lung fibrosis

Authors

Serena Janho dit Hreich[1,2], Thierry Juhel[1], Sylvie Leroy[2,3,4], Alina Ghinet[5,6,7], Frederic Brau[3], Véronique Hofman[1,2,8,9], Paul Hofman[1,2,8,9], Valérie Vouret-Craviari[1,2]

Affiliations

1. Université Côte d'Azur, CNRS, INSERM, IRCAN, 06108 Nice, France.
2. FHU OncoAge, Nice, France.
3. Université Côte d'Azur, CNRS, Institut Pharmacologie Moléculaire et Cellulaire, Sophia-Antipolis, France.
4. Université Côte d'Azur, Centre Hospitalier Universitaire de Nice, Pneumology Department, Nice, France.
5. Inserm U995, LIRIC, Université de Lille, CHRU de Lille, Faculté de médecine – Pôle recherche, Place Verdun, F-59045 Lille Cedex, France.
6. Hautes Etudes d'Ingénieur (HEI), JUNIA Hauts-de-France, UCLille, Laboratoire de chimie durable et santé, 13 rue de Toul, F-59046 Lille, France.
7. 'Al. I. Cuza' University of Iasi, Faculty of Chemistry, Bd. Carol I, nr. 11, 700506 Iasi, Romania.
8. Laboratory of Clinical and Experimental Pathology and Biobank, Pasteur Hospital, Nice, France.
9. Hospital-Related Biobank (BB-0033-00025), Pasteur Hospital, Nice, France.

Corresponding author: Valérie VOURET-CRAVIARI, IRCAN, 28 Avenue de Valombrose, 06108 Nice, France. Tel 33 (0)492031223. Email : valerie.vouret@univ-cotedazur.fr

Conflict of interest statement: All other authors declare they have no competing interests.

Abstract

Idiopathic pulmonary fibrosis (IPF) is an aggressive interstitial lung disease associated with progressive and irreversible deterioration of respiratory functions that lacks curative therapies. Despite IPF being associated with a dysregulated immune response, current antifibrotics aim only at limiting fibroproliferation. We show here that the *P2RX7/IL-18/IFNG* axis is downregulated in IPF patients and that P2RX7 has immunoregulatory functions. Using our positive modulator of P2RX7, we show that activation of the P2RX7/IL-18 axis in immune cells limits lung fibrosis progression in a mouse model by favoring an anti-fibrotic immune environment, with notably an enhanced IL-18-dependent IFN-γ production by lung T cells leading to a decreased production of IL-17 and TGFβ. Overall, we show the ability of the immune system to limit lung fibrosis progression by targeting the immunomodulator P2RX7. Hence, treatment with a small activator of P2RX7 may represent a promising strategy for patients with lung fibrosis.

Introduction

Idiopathic pulmonary fibrosis (IPF) is an aggressive interstitial lung disease associated with progressive deterioration of respiratory function that is ultimately fatal. It is characterized by destruction of the lung architecture due to accumulation of fibroblasts and extracellular matrix proteins, resulting in increased lung stiffness and impaired normal breathing.

Pirfenidone and nintedanib have been FDA approved for the treatment of IPF since 2014. They target respectively the key fibrotic cytokine TGFβ and several receptor tyrosine kinases, thereby affecting fibroblast activation and extracellular matrix protein production (1). However, they only slow down the progression of the disease, so new therapeutic strategies and targets are needed.

Fibrosis is also associated with inflammation. In fact, fibrosis is a process of excessive wound healing and tissue remodeling due to repeated epithelial injuries releasing damage-associated molecular patterns (DAMPs) that trigger both the adaptive and innate immune systems. Although inflammation has not been considered a target in IPF, due to unsuccessful initial clinical trials of anti-inflammatory drugs (2) or cyclophosphamide during exacerbations (3), growing evidence suggest that altering specific immune populations that promote or attenuate disease progression may be beneficial (4).

Extracellular adenosine triphosphate (eATP) is a DAMP, released in high concentrations from injured cells in IPF patients (5). High levels of eATP are recognized by the P2X7 receptor (P2RX7) and are both required for the establishment of the bleomycin lung fibrosis mouse model (5). Activation of P2RX7 induces the opening of macropores, resulting in cell death (6), but also leads to the assembly of the NLRP3 inflammasome and the release of mature IL-1β and IL-18 (7). Consequently, P2RX7 has the ability to trigger an immune response.

IL-1β is a proinflammatory cytokine with high profibrotic properties, as it promotes collagen deposition through IL-17A and TGFβ production (8–10) but also promotes the activation and

recruitment of inflammatory cells such as eosinophils and neutrophils. Indeed, deficiency of IL-1βR or its blockade ameliorate experimental fibrosis (11–13). In contrast, the role of IL-18 is not clear. Indeed, conflicting experimental studies show that IL-18 could either promote (14) or attenuate (15) fibrosis. However, high levels of IL-18BP, a natural antagonist of IL-18, are associated with reduced overall survival in IPF patients (16), suggesting that the activity of IL-18 may be required for improved survival.

IL-18 was originally described as IFN-γ-inducing factor (IGIF) and therefore boosts IFN-γ production by T cells and NK cells (17). Not only has IFN-γ antiproliferative properties (18) but it also inhibits TGFβ activity (19, 20) and therefore inhibits fibroblast activation and differentiation into myofibroblasts, alleviates TGFβ-mediated immunosuppression, inhibits extracellular matrix accumulation and collagen production (21–24) and thus promotes an antifibrotic immune microenvironment, making IFN-γ a cytokine with antifibrotic properties. However, parenteral systemic administration of IFN-γ failed in clinical trials (INSPIRE; NCT 00075998) (25), whereas local administration by inhalation showed promising results (26–30).

One way to increase IFN-γ production locally and selectively in the lung would be to alter the phenotype of T cells since the polarization of T lymphocytes has been shown to impact fibroblasts' fate and immune infiltrate (4, 31). Indeed, T cells have been recently shown to selectively kill myofibroblasts through IFN-γ release and limit the progression of lung and liver fibrosis in preclinical models (32) and set up an immune memory in the long term since IFN-γ-producing tissue resident memory T cells protect against fibrosis progression (33), highlighting the importance IFN-γ producing T cells in this disease. Accordingly, $CD4^+$-producing IFN-γ T cells are decreased in IPF and correlate with a better prognosis in IPF patients (31, 34, 35).

Given the ability of IL-18 to shape the phenotype of T cells by inducing IFN-γ, we proposed to increase local IFN-γ production via the P2RX7/IL-18 axis as a therapeutic strategy in pulmonary fibrosis. We used a P2RX7-specific positive modulator, developed in our

laboratory, which has the particularity to only increase IL-18 levels in the presence of high eATP (36).

Results

Expression of P2RX7 and IL-18 activity are dampened in IPF patients

The canonical release of IL-18 is due to activation of the P2RX7/NLRP3 pathway (*7*). Since high levels of eATP are found in IPF patients (5) and P2RX7 is activated by such levels, it was of particular interest to investigate the involvement of P2RX7 in this disease. We used a publicly available dataset of lung homogenates from control and IPF patients (GSE47460) and compared the expression levels of P2RX7 and markers of fibrosis, namely *ACTA2*, *COL1A2*, *COL3A1* and *TGFB3*. We found that the expression of P2RX7 is downregulated in IPF patients (Figure 1A and B), as well as the components of the NLRP3 inflammasome (Supplemental Figure 1). Since IL-18 is constitutively expressed (37), which partly explains the lack of difference between control and IPF patients (Figure 1B), we investigated the signaling pathway downstream of IL-18. IL-18 binds to its receptor IL-18R1 coupled to its adaptor protein IL-18RAP which is required for IL-18 signaling and IFN-γ expression. We showed that *IL-18R1*, *IL-18RAP* and *IFN-γ* (Figure 1B) are downregulated in IPF patients. Knowing that the modulation of the phenotype of T cells is promising in IPF (4), we checked whether P2RX7 and IL-18 are linked to an immune response in IPF using Gene Set Enrichment Analyses. Indeed, we showed that the expression of P2RX7 and IL-18 signaling (IL-18 and IL-18RAP) correlates with the IFN-γ response as well as with immunoregulatory interactions required for changing the phenotype of T cells (Figure 1C, Supplemental Figure 1B). These results highlight that the P2RX7/IL-18 signaling pathway is dampened and that this pathway is able to modulate the immune response in IPF patients.

Activation of P2RX7 inhibits the onset of pulmonary fibrosis in the bleomycin mouse model

We therefore hypothesized that activation of the P2RX7/IL-18 signaling may restrain lung fibrosis progression. To test this hypothesis, we decided to boost the P2RX7/IL-18 signaling in

the bleomycin (BLM)-induced lung fibrosis mouse model. To do so, we used a positive modulator of P2RX7, called HEI3090, which enhances P2RX7's activity only in the presence of high eATP levels (36). Indeed, knowing that high eATP levels are found in IPF patients as well as in this mouse model of pulmonary fibrosis (5), we thought that HEI3090 will selectively enhance the activity of P2RX7 in the lungs.

We first tested the antifibrotic potential of HEI3090 on mice having an established fibrosis (Figure 2A). Activation of P2RX7 with HEI3090 in mice 7 days after BLM administration reduced the development of pulmonary fibrosis, as evidenced by less thickening of alveolar walls and free air space (Figure 2B). Fibrosis severity was evaluated using the Ashcroft score. To overcome the heterogeneity of fibrosis within the lobes, we scored the whole surface of the lung, and the result represents the mean of each field (Figure 2C and supplementary Figure 2). As accumulation of extracellular matrix proteins is a hallmark of fibrosis, we also checked collagen levels in the lungs of vehicle and HEI3090-treated mice by measuring Sirius Red polarized light images of the entire lung. We showed that collagen content was reduced in lungs of HEI3090-treated mice (Figure 2, B and D). We also tested the ability of HEI3090 to limit lung fibrosis progression when administered during the inflammatory phase of the BLM model (Figure 2E) that mimics the exacerbation episodes in IPF patients (38). HEI3090 was also able to inhibit the onset of lung fibrosis in this setting given the reduced fibrosis score (Figure 2, F and J) and collagen content in lungs of HEI3090-treated mice (Figure 2, F and H). These results show that activation of P2RX7 with HEI3090 inhibits the lung fibrosis progression and is effective during both the fibroproliferative and acute inflammation phase of the BLM-induced pulmonary fibrosis mouse model.

HEI3090 shapes immune cell infiltration in the lungs

As P2RX7 has immunoregulatory functions in IPF (Figure 1) and as HEI3090 has antifibrotic activity (Figure 2), we next investigated if HEI3090 had an impact on both the immune

landscape of the lung and production of cytokines. We show that lung CD3+ T cells were more biased to produce IFN-γ than the profibrotic IL-17A cytokine when mice were treated with HEI3090 (Figure 3A). This result is consistent with what we have shown in IPF patients (Figure 1). This biased production of IFN-γ is only seen in CD3+ T cells and not in overall lung immune cells (Supplemental Figure 3A) nor in the subsets of T lymphocytes (Figure 3B, Supplemental Figure 3A) or NK cells (Supplemental Figure 3B). Although levels of CD3+ T cells and T cell subsets were unchanged (Supplemental Figure 3C), including the profibrotic Th17 cells (Figure 3D), IL-17A production by Th17 cells is markedly attenuated after HEI3090 treatment (Figure 3D), consistent with the ability of IFN-γ to inhibit IL-17A production (39). Considering the strong profibrotic properties of TGFβ and its mutual antagonism with IFN-γ (40, 41), we checked whether HEI3090 had an effect on TGFβ levels. Indeed, treatment with HEI3090 reduced TGFβ-producing immune cells in the lung as well as TGFβ production (Figure 3E). Notably, HEI3090 treatment reduced TGFβ production in NK cells but not in T-cell subsets (Supplemental Figure 3E).

Pulmonary fibrosis is also favored and driven by the recruitment of inflammatory cells, mainly from the myeloid lineage. Monocytes are highly inflammatory cells that are recruited to the lung and differentiate into alveolar macrophages, both of which have strong profibrotic properties (42–44). We demonstrated that in HEI3090-treated mice, the number of inflammatory monocytes decreased markedly (Figure 3E), whereas the number of alveolar macrophages remained unchanged (Figure 3F), consistent with the prognostic ability of monocyte count in IPF progression (45–48). We also examined other inflammatory cells with profibrotic properties, such as eosinophils (49) that are less present in HEI3090-treated lungs (Figure 3G), or PMN levels that remain unchanged by HEI3090 treatment (Supplemental Figure 3C).

We also wondered if the activation of P2RX7 had a systemic effect by analyzing immune changes in mice's spleens. No significant change in cell populations was observed in the spleens of mice (Supplemental Figure 4B) when HEI3090 was administrated in the early phase of the BLM model suggesting a local lung activity of the molecule. However, HEI3090 reactivated a systemic immune response with higher levels of dendritic cells and lymphocytes in the spleens of mice treated during the fibroproliferation phase (Supplemental Figure 4D). These results show the ability of HEI3090 to shape the immune response locally and impact the progression of fibrosis systemically even in the fibroproliferative phase of the BLM model.

Altogether these results demonstrate that activation of P2RX7 with HEI3090 promotes an antifibrotic cytokinic profile in lung immune cells and attenuates lung inflammation.

HEI3090 requires the P2RX7/NLRP3/IL-18 pathway in immune cells to inhibit lung fibrosis

We wanted to further investigate the mechanism of action of HEI3090 by identifying the cellular compartment and signaling pathway required for its activity. Since the expression of P2RX7 and the P2RX7-dependent release of IL-18 are mostly associated with immune cells(50), and since HEI3090 shapes the lung immune landscape (Figure 3), we investigated whether immune cells were required for the antifibrotic effect of HEI3090.

To do so, we performed an adoptive transfer experiment with WT P2RX7-expressing splenocytes (Figure 4A, supplemental Figure 5E) into *p2rx7*$^{-/-}$ mice one day before BLM administration. We show that restriction of P2RX7 expression on immune cells restored the antifibrotic effect of HEI3090 based on the architecture of the lung, with lungs of HEI3090-treated mice showing more free airspace and thinner alveolar walls (Figure 4B), as well as an overall lower fibrosis score (Figure 4C) than control lungs. Since the bleomycin mouse model relies on P2RX7-expressing epithelial cells (5), we wanted to validate further the role of

P2RX7-expressing immune cells in a mouse model where P2RX7 is expressed by non-immune cells. To do so, we reduced both the expression of P2RX7 and its activity by repeated i.v. administration of *p2rx7*$^{-/-}$ splenocytes in WT mice (Supplemental Figure 5). In this setting, HEI3090 was unable to limit the progression of fibrosis. Moreover, we show that the activity of HEI3090 requires P2RX7 expression, as this effect was lost in *p2rx7*$^{-/-}$ mice (Supplemental Figure 6, A and B) (36). These results highlight the important role of immune cells and rules out a major role of non-immune P2RX7-expressing cells, such as fibroblasts, in the antifibrotic effect of HEI3090.

To test the importance of the NLRP3/IL-18 pathway downstream of P2RX7, we performed an adoptive transfer of *nlrp3*$^{-/-}$ and *il18*$^{-/-}$ splenocytes into *p2rx7*$^{-/-}$ mice, expressing similar levels of P2RX7 as WT splenocytes (Supplemental Figure 6E), but also the same levels of IL-18 and NLRP3 (Supplemental Figure 6F). The absence of NLRP3 and IL-18 in P2RX7-expressing immune cells abrogated the ability of HEI3090 to inhibit lung fibrosis because the lung architecture resembled that of control mice (Figure 4, D-G). Consistent with the requirement of IL-18 for HEI3090's antifibrotic activity, activation of P2RX7 with this molecule in WT mice increased the levels of IL-18 in the sera of these mice compared to control mice (Figure 4H). Moreover, neutralization of IL-18 abrogated the increase of the IFN-γ/IL-17A ratio by lung T cells (Figure 4I), highlighting furthermore the necessity of IL-18 for the antifibrotic effect of HEI3090.

Not only does the activation of the P2RX7/NLRP3 pathway leads to the release of IL-18, but also induce the release of the pro-inflammatory and pro-fibrotic IL-1β cytokine. However, IL-1β was not involved in the antifibrotic effect of HEI3090 (Supplemental Figure 6C), nor were its levels affected by HEI3090 in WT mice (Supplemental Figure 6D).

Overall, we show that the P2RX7/NLRP3/IL-18 axis in immune cells is required to limit lung fibrosis progression, highlighting the efficacy in targeting the immune system in this disease.

Discussion

A major unmet need in the field of IPF is new treatment to fight this uncurable disease. In this study, we demonstrate the ability of immune cells to limit lung fibrosis progression. Based on the hypothesis that a local activation of a T cell immune response and upregulation of IFN-γ production has antifibrotic proprieties, we used the HEI3090 positive modulator of the purinergic receptor P2RX7, previously developed in our laboratory (36), to demonstrate that activation of the P2RX7/IL-18 pathway inhibits lung fibrosis in the bleomycin mouse model.

We have demonstrated that lung fibrosis progression is inhibited by HEI3090 in the fibrotic phase but also in the acute phase of the BLM fibrosis mouse model, i.e. during the period of inflammation. This lung fibrosis mouse model is classically used in preclinical studies and has been designated recently as the best model for IPF (51). The efficacy of HEI3090 to inhibit lung fibrosis was evaluated histologically on the whole lung's surface by evaluating the severity of fibrosis and collagen levels using respectively the Ashcroft score (52) and polarized-light microscopy of Sirius Red staining to visualize collagen fibers in the whole lung. In both settings, HEI3090 reduced alveolar wall thickness and accumulation of collagen fibers in the entire lung, highlighting a comprehensive pre-clinical evaluation of HEI3090 as a new anti-fibrotic therapy.

Our study showed that inhibition of fibrosis progression by HEI3090 was associated with an increased production of IFN-γ by lung T cells that was dependent on an increased release of IL-18. We also showed that expression of the P2RX7/IL-18/IFN-γ pathway is attenuated in IPF patients where TGFβ levels are high (52), consistent with the ability of TGFβ to downregulate IL-18R expression and IL-18-mediated IFN-γ production (53). These results confirm the beneficial effects of enhancing activation of the P2RX7/IL-18/IFN-γ pathway.

P2RX7 is expressed by various immune and non-immune cells, but its expression is the highest in dendritic cells (DCs) and macrophages (54), from which IL-18 is mainly released to shape

the T-cell response (55) and increase T-cell IFN-γ production (56). Collectively, and consistent with the immunomodulatory properties of P2RX7, these observations suggest that HEI3090 may target P2RX7-expressing antigen-presenting cells to influence the T-cell response, which may explain the selective T-cell increase in IFN-γ in HEI3090-treated mice. Accordingly, we have previously shown that HEI3090 targets the P2RX7/IL-18 axis in DCs to shape the immune response in a lung tumor mouse model (36).

Activation of P2RX7 with HEI3090 not only increased IFN-γ production by T cells but it also reshaped the immune and cytokinic composition of the lung. Indeed, lungs of HEI3090-treated mice show a decrease in IL-17A production by Th17 cells and TGFβ production by lung immune cells. Moreover, lung inflammation is dampened after HEI3090 treatment, since the number of inflammatory monocytes and eosinophils decreases. It is not known whether this cytokinic and anti-inflammatory switch is solely due to the IL-17A and TGFβ-suppressive property of IFN-γ (57–59), or whether it is a combination with the cell death-inducing property of P2RX7 (6).

The novelty of this approach is that it targets and alters the immune environment of the lung. Indeed, the use of a P2RX7-specific modulator that acts only in an ATP-rich environment was effective in promoting an anti-inflammatory and anti-fibrotic phenotype by altering several key mediators of the disease. In contrast to current therapies (60), no side effects were observed when mice were treated with HEI3090, further supporting this targeted approach. Furthermore, since current therapies (pirfenidone or nintedanib) and HEI3090 have different mechanisms of action, the combination of these therapies could have additive or synergistic effects.

It is also important to note that our strategy is unconventional, as P2RX7 is known to be pro-inflammatory through IL-1β-release. However, HEI3090 was unable to increase IL-1β release *in vivo* in this model, even though it efficiently increased IL-18 release. This observation is consistent with our previous *in vivo* and *in vitro* studies (36), allowing us to rule out the pro-

inflammatory and pro-fibrotic effects of P2RX7-dependent IL-1β release. Consistent with this finding, it has been reported that ATP stimulation of alveolar macrophages derived from both IPF and lung cancer patients resulted only in an increase in IL-18 (61, 62), which was explained by an impaired NLRP3 inflammasome and a defective autophagy described in IPF patients (63). Interestingly, autophagy can be regulated by P2RX7 (64) and is one of the pathways that allow the release of IL-1β from the cell (65). Moreover, unlike IL-1β, IL-18 is constitutively expressed in human and mouse immune cells (37) but also in non-immune cells such as fibroblasts (66) and lung epithelium (67) and is both matured and released after NLRP3 activation. Therefore, it is currently not known whether the lack of IL-1β release is due to the different cytokine expression pattern or whether there is IL-1β-specific regulation following an enhanced activation of P2RX7 or a defective NLRP3 inflammasome.

In this study, we emphasize the importance of IL-18 for an antifibrotic effect. Several studies have indicated that P2RX7/NLRP3/IL-18 promote disease progression using knock out mice or inhibitors (5, 14, 66). However, experimental mouse models rely on lung epithelial cell injury that has been shown to activate the NLRP3 inflammasome in the lung epithelium as a first step (5, 12) and release danger signals that activate the immune system as a second step. Therefore, initial lung injury to epithelial cells is reduced or absent in *p2rx7*$^{-/-}$ and *nlrp3*$^{-/-}$ mice, indicating that P2RX7 and NLRP3 are required for the establishment of the bleomycin mouse model rather than their role in an already established fibrosis, which has not yet been studied. In addition, NLRP3 and the release of IL-1β and IL-18 from fibroblasts have been shown to promote myofibroblast differentiation and extracellular matrix production (66, 68, 69). These observations suggest that fibrosis mouse models initially rely on NLRP3 activation by nonimmune cells and encourage further studies on the contribution of the NLRP3 inflammasome in immune cells to fibrosis progression *in vivo*. Since we have highlighted the

importance of this pathway in immune cells for delaying fibrosis progression, we propose that IL-18 may have different effects depending on the cell type.

Beside an urgent need of new treatments for IPF, there is also a lack of biomarkers, such as prognostic biomarkers, markers of disease activity, or markers of drug efficacy. Our results suggest the possible benefit of an active IL-18 in the pathophysiology of pulmonary fibrosis and warrant analysis of IL-18 as a promising biomarker for predicting outcome in IPF patients. Given the potential effects of pirfenidone and nintedanib on IL-18 levels in preclinical models (70–72), determining IL-18 shifts during treatment would be highly interesting to evaluate potential changes in patients' outcome and to examine IL-18 levels which may be helpful in the long run for patient treatment strategy and subsequent introduction of pipeline drugs (73).

Overall, we highlight in this study the ability of the P2RX7/NLRP3/IL-18 pathway in immune cells to inhibit the onset of lung fibrosis by using a positive modulator of P2RX7 that acts selectively in an eATP-rich environment such as fibrotic lung. The unique feature of this strategy is that it enhances the antifibrotic and it attenuates the pro-fibrotic properties of immune cells, with no reported side effects.

Methods

Microarray

mRNA expression profile was obtained from Gene Expression Omnibus (GEO) database (GSE47460) using the GPL14550. Microarray was done on whole lung homogenate from subjects undergoing thoracic surgery from healthy subjects with no lung-related pathology or from subjects diagnosed as having interstitial lung disease as determined by clinical history, CT scan, and surgical pathology. Expression profile belong to the Lung Tissue Research Consortium (LTRC). 122 patients with UIP/IPF and 91 healthy controls were analyzed in this study.

Mice

Mice were housed under standardized light–dark cycles in a temperature-controlled air-conditioned environment under specific pathogen-free conditions at IRCAN, Nice, France, with free access to food and water. All mouse studies were approved by the committee for Research and Ethics of the local authorities (CIEPAL #598, protocol number APAFIS 21052-2019060610506376) and followed the European directive 2010/63/UE, in agreement with the ARRIVE guidelines. Experiments were performed in accord with animal protection representative at IRCAN. *p2rx7*$^{-/-}$ (B6.129P2-P2rx7tm1Gab/J, from the Jackson Laboratory) were backcrossed with C57BL/6J OlaHsD mice. C57BL/6J OlaHsD male mice (WT) were supplied from Envigo (Gannat, France).

Induction of lung fibrosis

WT or *p2rx7*$^{-/-}$ male mice (8 weeks) were anesthetized with ketamine (25mg/kg) and xylazine (2.5 mg/kg) under light isoflurane and were given 2.5 U/kg of bleomycin sulfate (Sigma-Aldrich) by intranasal route. Mice were treated i.p. every day with vehicle (PBS, 10% DMSO) or with HEI3090 (1.5 mg/kg in PBS, 10% DMSO) (*36*) starting D1 or D7 post bleomycin

delivery, as mentioned in the figures. After 14 days of treatment, lungs were either fixed for paraffin embedding or weighted and analyzed by flow cytometry. When mentioned, 200 µg of anti-IL-18 neutralizing antibody (BioXcell) or isotype control (IgG2a, BioXcell) were given by i.p. every three days starting one day prior to BLM administration.

Adoptive transfer in *p2rx7* deficient mice

Spleens from C57BL/6J male mice (8-10 weeks) were collected and digested with the spleen dissociation kit (Miltenyi Biotech) according to the supplier's instructions. 3.10^6 splenocytes were injected i.v. in *p2rx7*$^{-/-}$ mice 1 day before intranasal delivery of bleomycin. Mice were treated i.p. every day for 14 days with vehicle (PBS, 10% DMSO) or with HEI3090 (1.5 mg/kg in PBS, 10% DMSO). *Nlrp3*$^{-/-}$ spleens were a kind gift from Dr Laurent Boyer, *il18*$^{-/-}$ spleens from Dr George Birchenough and *il1b*$^{-/-}$ spleens from Dr Bernhard Ryffel, all on a C57BL/6J background.

Histology

Lungs were collected and fixed in 3% formamide for 16 h prior inclusion in paraffin. Lungs sections (3 µm) were stained with hematoxylin & eosin or with Sirius red (Abcam) according to the supplier's instructions. The severity of fibrosis was assessed on whole lungs using the Ashcroft modified method (74). The fibrosis score represents the mean of fields of 0.883 mm^2 each covering all the lobes of the lungs as shown in Supplementary Figure 2.

Levels of collagen on whole lungs were assessed on Sirius Red polarized light images of the entire lung taken with HD - Axio Observer Z1 Microscope ZEISS microscope using ImageJ. The collagen amount given by the polarization intensity of the Sirius red staining of the lung slices was quantified with a homemade ImageJ/Fiji (75) macro program. The mean gray value of the collagen staining was measured in the fibrotic regions excluding the signal coming from vessels and lung epithelia using dedicated masks. The binary masks were obtained after median

filtering and manual thresholding, from the transmission images for the fibrotic one and the polarization images for the vessels. The intersection of these masks is then applied on the polarization image to get specifically the mean gray value of fibrotic collagen.

Flow cytometry and antibodies

Lungs or spleens were collected and digested with the lung or spleen dissociation kit (Miltenyi Biotech) according to the supplier's instructions. Red blood cells were lysed using ACK lysis buffer (Gibco). Fc receptors were blocked using anti-CD16/32 (2.4G2) antibodies followed by surface staining by incubating cells on ice, for 20 min, with saturating concentrations of labeled Abs (Table 1) in PBS, 5% FBS and 0.5% EDTA. Tregs were identified using the transcription factor staining Buffer Set (eBioscience) for FoxP3 staining. Intracellular staining was performed after stimulation of single-cell suspensions with Phorbol 12-myristate 13-acetate (PMA at 50 ng mL^{-1}, Sigma), ionomycin (0.5 µg mL^{-1}, Sigma) and 1 µL mL^{-1} Golgi Plug™ (BD Biosciences) for 4 h at 37°C 5% CO_2. Cells were incubated with Live/Dead stain (Invitrogen), according to the manufacturer protocol prior to surface staining. Intracellular staining was performed using Cytofix/Cytoperm™ kit (BD biosciences) following the manufacturer's instructions. Samples were acquired on CytoFLEX LX (Beckman Coulter) and analyzed using FlowJo (LLC).

ELISA

Sera of mice were collected at the end of the experiment and stored at −80 °C before cytokine detection by ELISA using mouse IL-1 beta/IL-1F2 (R&D) and IL-18 (MBL) according to the supplier's instructions.

Western Blot

Single cell suspensions of whole lungs were lysed with Laemmli buffer (10% glycerol, 3% SDS, 10 mM Na2HPO4) with protease inhibitor cocktail (Roche). Proteins were separated on

a 12% SDS-PAGE gel and electro transferred onto PVDF membranes, which were blocked for 30 min at RT with 3% bovine serum albumin or 5% milk. Membranes were incubated with primary antibodies (see Table 1) diluted at 4 °C overnight. Secondary antibodies (Promega) were incubated for 1 h at RT. Immunoblot detection was achieved by exposure with a chemiluminescence imaging system (PXI Syngene, Ozyme) after membrane incubation with ECL (Immobilon Western, Millipore). The bands intensity values were normalized to that of β-actin using ImageJ software.

Statistical analyses

All analyses were carried out using Prism software (GraphPad). Mouse experiments were performed on at least n = 5 individuals, as indicated. Mice were equally divided for treatments and controls. Data is represented as mean values and error bars represent SEM. Two-tailed Mann–Whitney and unpaired t-test were used to evaluate the statistical significance between groups. For survival analyses, the log-rank Mantel-Cox test was used. For correlation analyses, Spearman test was used for the Gene Set Enrichment Analyses (GSEA).

Data and materials availability: All data are available in the main text or the supplementary materials. RNAseq data from IPF and control patients were retrieved from GEO database under the accession number GSE47460.

Author contributions:

Conceptualization and design: SJH, VV-C

Methodology: SJH, FB

Investigation: SJH, TJ, VV-C

Analysis and Interpretation: SJH, SL, PH, VH, VV-C

Reagents: AG

Writing: SJH, VV-C

Acknowledgments

The authors wish to thank Dr George Birchenough, Dr Laurent Boyer and Dr Bernhard Ryffel for sharing *il18*$^{-/-}$, *nlrp3*$^{-/-}$ and *il1b*$^{-/-}$ spleens respectively. This publication is based upon discussion from PRESTO COST action CA21130 supported by COST (European Cooperation in Science and Technology).

Funding: Ligue Nationale Contre le Cancer (SJH), Fondation pour la recherche médicale grant number #FDT202106013099 (SJH), ARC grant number ARCTHEM2021020003478 (SJH, VV-C), Cancéropôle PACA (VV-C)

The French Government (National Research Agency, ANR through the "Investments for the Future": program reference #ANR-11-LABX-0028-01 (PH), Executive Unit for Financing Higher Education, Research, Development and Innovation (UEFISCDI), Bucharest, Romania (grant number PN-III-P4-ID-PCE-2020-0818, acronym REPAIR) (AG).

References

1. P. Heukels, C. C. Moor, J. H. von der Thüsen, M. S. Wijsenbeek, M. Kool, Inflammation and immunity in IPF pathogenesis and treatment. *Respir Med*. **147**, 79–91 (2019).

2. Idiopathic Pulmonary Fibrosis Clinical Research Network, G. Raghu, K. J. Anstrom, T. E. King, J. A. Lasky, F. J. Martinez, Prednisone, azathioprine, and N-acetylcysteine for pulmonary fibrosis. *N Engl J Med*. **366**, 1968–77 (2012).

3. J.-M. Naccache, S. Jouneau, M. Didier, R. Borie, M. Cachanado, A. Bourdin, M. Reynaud-Gaubert, P. Bonniaud, D. Israël-Biet, G. Prévot, S. Hirschi, F. Lebargy, S. Marchand-Adam, N. Bautin, J. Traclet, E. Gomez, S. Leroy, F. Gagnadoux, F. Rivière, E. Bergot, A. Gondouin, E. Blanchard, A. Parrot, F.-X. Blanc, A. Chabrol, S. Dominique, A. Gibelin, A. Tazi, L. Berard, P. Y. Brillet, M.-P. Debray, A. Rousseau, M. Kerjouan, O. Freynet, M.-C. Dombret, A.-S. Gamez, A. Nieves, G. Beltramo, J. Pastré, A. Le Borgne-Krams, T. Dégot, C. Launois, L. Plantier, L. Wémeau-Stervinou, J. Cadranel, C. Chenivesse, D. Valeyre, B. Crestani, V. Cottin, T. Simon, H. Nunes, Cyclophosphamide added to glucocorticoids in acute exacerbation of idiopathic pulmonary fibrosis (EXAFIP): a randomised, double-blind, placebo-controlled, phase 3 trial. *Lancet Respir Med*. **10**, 26–34 (2022).

4. K. Shenderov, S. L. Collins, J. D. Powell, M. R. Horton, Immune dysregulation as a driver of idiopathic pulmonary fibrosis. *J Clin Invest*. **131** (2021), doi:10.1172/JCI143226.

5. N. Riteau, P. Gasse, L. Fauconnier, A. Gombault, M. Couegnat, L. Fick, J. Kanellopoulos, V. F. J. Quesniaux, S. Marchand-Adam, B. Crestani, B. Ryffel, I. Couillin, Extracellular ATP is a danger signal activating P2X7 receptor in lung inflammation and fibrosis. *Am J Respir Crit Care Med*. **182**, 774–83 (2010).

6. A. Surprenant, F. Rassendren, E. Kawashima, R. A. North, G. Buell, The cytolytic P2Z receptor for extracellular ATP identified as a P2X receptor (P2X7). *Science*. **272**, 735–8 (1996).

7. D. G. Perregaux, P. McNiff, R. Laliberte, M. Conklyn, C. A. Gabel, ATP acts as an agonist to promote stimulus-induced secretion of IL-1 beta and IL-18 in human blood. *J Immunol*. **165**, 4615–23 (2000).

8. M. S. Wilson, S. K. Madala, T. R. Ramalingam, B. R. Gochuico, I. O. Rosas, A. W. Cheever, T. A. Wynn, Bleomycin and IL-1beta-mediated pulmonary fibrosis is IL-17A dependent. *J Exp Med*. **207**, 535–52 (2010).

9. C. E. Sutton, S. J. Lalor, C. M. Sweeney, C. F. Brereton, E. C. Lavelle, K. H. G. Mills, Interleukin-1 and IL-23 induce innate IL-17 production from gammadelta T cells, amplifying Th17 responses and autoimmunity. *Immunity*. **31**, 331–41 (2009).

10. A. M. Doerner, B. L. Zuraw, TGF-beta1 induced epithelial to mesenchymal transition (EMT) in human bronchial epithelial cells is enhanced by IL-1beta but not abrogated by corticosteroids. *Respir Res*. **10**, 100 (2009).

11. I. Couillin, V. Vasseur, S. Charron, P. Gasse, M. Tavernier, J. Guillet, V. Lagente, L. Fick, M. Jacobs, F. R. Coelho, R. Moser, B. Ryffel, IL-1R1/MyD88 signaling is critical for elastase-induced lung inflammation and emphysema. *J Immunol*. **183**, 8195–202 (2009).

12. P. Gasse, N. Riteau, S. Charron, S. Girre, L. Fick, V. Pétrilli, J. Tschopp, V. Lagente, V. F. J. Quesniaux, B. Ryffel, I. Couillin, Uric acid is a danger signal activating NALP3 inflammasome in lung injury inflammation and fibrosis. *Am J Respir Crit Care Med*. **179**, 903–13 (2009).

13. P. Gasse, C. Mary, I. Guenon, N. Noulin, S. Charron, S. Schnyder-Candrian, B. Schnyder, S. Akira, V. F. J. Quesniaux, V. Lagente, B. Ryffel, I. Couillin, IL-1R1/MyD88

signaling and the inflammasome are essential in pulmonary inflammation and fibrosis in mice. *J Clin Invest*. **117**, 3786–99 (2007).

14. L.-M. Zhang, Y. Zhang, C. Fei, J. Zhang, L. Wang, Z.-W. Yi, G. Gao, Neutralization of IL-18 by IL-18 binding protein ameliorates bleomycin-induced pulmonary fibrosis via inhibition of epithelial-mesenchymal transition. *Biochem Biophys Res Commun*. **508**, 660–666 (2019).

15. A. Nakatani-Okuda, H. Ueda, S.-I. Kashiwamura, A. Sekiyama, A. Kubota, Y. Fujita, S. Adachi, Y. Tsuji, T. Tanizawa, H. Okamura, Protection against bleomycin-induced lung injury by IL-18 in mice. *Am J Physiol Lung Cell Mol Physiol*. **289**, L280-7 (2005).

16. Y. Nakanishi, Y. Horimasu, K. Yamaguchi, S. Sakamoto, T. Masuda, T. Nakashima, S. Miyamoto, H. Iwamoto, S. Ohshimo, K. Fujitaka, H. Hamada, N. Hattori, IL-18 binding protein can be a prognostic biomarker for idiopathic pulmonary fibrosis. *PLoS One*. **16**, e0252594 (2021).

17. H. Okamura, H. Tsutsi, T. Komatsu, M. Yutsudo, A. Hakura, T. Tanimoto, K. Torigoe, T. Okura, Y. Nukada, K. Hattori, Cloning of a new cytokine that induces IFN-gamma production by T cells. *Nature*. **378**, 88–91 (1995).

18. J. A. Elias, S. A. Jimenez, B. Freundlich, Recombinant gamma, alpha, and beta interferon regulation of human lung fibroblast proliferation. *Am Rev Respir Dis*. **135**, 62–5 (1987).

19. L. Ulloa, J. Doody, J. Massagué, Inhibition of transforming growth factor-beta/SMAD signalling by the interferon-gamma/STAT pathway. *Nature*. **397**, 710–3 (1999).

20. J. Varga, A. Olsen, J. Herhal, G. Constantine, J. Rosenbloom, S. A. Jimenez, Interferon-gamma reverses the stimulation of collagen but not fibronectin gene expression by transforming growth factor-beta in normal human fibroblasts. *Eur J Clin Invest*. **20**, 487–93 (1990).

21. G. Gurujeyalakshmi, S. N. Giri, Molecular mechanisms of antifibrotic effect of interferon gamma in bleomycin-mouse model of lung fibrosis: downregulation of TGF-beta and procollagen I and III gene expression. *Exp Lung Res*. **21**, 791–808.

22. P. Gillery, H. Serpier, M. Polette, G. Bellon, C. Clavel, Y. Wegrowski, P. Birembaut, B. Kalis, R. Cariou, F. X. Maquart, Gamma-interferon inhibits extracellular matrix synthesis and remodeling in collagen lattice cultures of normal and scleroderma skin fibroblasts. *Eur J Cell Biol*. **57**, 244–53 (1992).

23. M. R. Duncan, B. Berman, Gamma interferon is the lymphokine and beta interferon the monokine responsible for inhibition of fibroblast collagen production and late but not early fibroblast proliferation. *J Exp Med*. **162**, 516–27 (1985).

24. W. Yuan, T. Yufit, L. Li, Y. Mori, S. J. Chen, J. Varga, Negative modulation of alpha1(I) procollagen gene expression in human skin fibroblasts: transcriptional inhibition by interferon-gamma. *J Cell Physiol*. **179**, 97–108 (1999).

25. T. E. King, C. Albera, W. Z. Bradford, U. Costabel, P. Hormel, L. Lancaster, P. W. Noble, S. A. Sahn, J. Szwarcberg, M. Thomeer, D. Valeyre, R. M. du Bois, INSPIRE Study Group, Effect of interferon gamma-1b on survival in patients with idiopathic pulmonary fibrosis (INSPIRE): a multicentre, randomised, placebo-controlled trial. *Lancet*. **374**, 222–8 (2009).

26. K. T. Diaz, S. Skaria, K. Harris, M. Solomita, S. Lau, K. Bauer, G. C. Smaldone, R. Condos, Delivery and safety of inhaled interferon-γ in idiopathic pulmonary fibrosis. *J Aerosol Med Pulm Drug Deliv*. **25**, 79–87 (2012).

27. G. C. Smaldone, Repurposing of gamma interferon via inhalation delivery. *Adv Drug Deliv Rev*. **133**, 87–92 (2018).

28. S. D. Skaria, J. Yang, R. Condos, G. C. Smaldone, Inhaled Interferon and Diffusion Capacity in Idiopathic Pulmonary Fibrosis (IPF). *Sarcoidosis Vasc Diffuse Lung Dis*. **32**, 37–42 (2015).

29. T. Fusiak, G. C. Smaldone, R. Condos, Pulmonary Fibrosis Treated with Inhaled Interferon-gamma (IFN-γ). *J Aerosol Med Pulm Drug Deliv*. **28**, 406–10 (2015).

30. C. Prior, P. L. Haslam, In vivo levels and in vitro production of interferon-gamma in fibrosing interstitial lung diseases. *Clin Exp Immunol*. **88**, 280–7 (1992).

31. I. G. Luzina, N. W. Todd, A. T. Iacono, S. P. Atamas, Roles of T lymphocytes in pulmonary fibrosis. *J Leukoc Biol*. **83**, 237–44 (2008).

32. M. Sobecki, J. Chen, E. Krzywinska, S. Nagarajan, Z. Fan, E. Nelius, J. M. Monné Rodriguez, F. Seehusen, A. Hussein, G. Moschini, E. Y. Hajam, R. Kiran, D. Gotthardt, J. Debbache, C. Badoual, T. Sato, T. Isagawa, N. Takeda, C. Tanchot, E. Tartour, A. Weber, S. Werner, J. Loffing, L. Sommer, V. Sexl, C. Münz, C. Feghali-Bostwick, E. Pachera, O. Distler, J. Snedeker, C. Jamora, C. Stockmann, Vaccination-based immunotherapy to target profibrotic cells in liver and lung. *Cell Stem Cell*. **29**, 1459-1474.e9 (2022).

33. S. L. Collins, Y. Chan-Li, M. Oh, C. L. Vigeland, N. Limjunyawong, W. Mitzner, J. D. Powell, M. R. Horton, Vaccinia vaccine–based immunotherapy arrests and reverses established pulmonary fibrosis. *JCI Insight*. **1** (2016), doi:10.1172/jci.insight.83116.

34. J. Xu, A. L. Mora, J. LaVoy, K. L. Brigham, M. Rojas, Increased bleomycin-induced lung injury in mice deficient in the transcription factor T-bet. *Am J Physiol Lung Cell Mol Physiol*. **291**, L658-67 (2006).

35. S. N. Giri, D. M. Hyde, B. J. Marafino, Ameliorating effect of murine interferon gamma on bleomycin-induced lung collagen fibrosis in mice. *Biochem Med Metab Biol*. **36**, 194–7 (1986).

36. L. Douguet, S. Janho Dit Hreich, J. Benzaquen, L. Seguin, T. Juhel, X. Dezitter, C. Duranton, B. Ryffel, J. Kanellopoulos, C. Delarasse, N. Renault, C. Furman, G. Homerin, C. Féral, J. Cherfils-Vicini, R. Millet, S. Adriouch, A. Ghinet, P. Hofman, V. Vouret-Craviari, A small-molecule P2RX7 activator promotes anti-tumor immune responses and sensitizes lung tumor to immunotherapy. *Nat Commun*. **12**, 653 (2021).

37. A. J. Puren, G. Fantuzzi, C. A. Dinarello, Gene expression, synthesis, and secretion of interleukin 18 and interleukin 1beta are differentially regulated in human blood mononuclear cells and mouse spleen cells. *Proc Natl Acad Sci U S A*. **96**, 2256–61 (1999).

38. R. Peng, S. Sridhar, G. Tyagi, J. E. Phillips, R. Garrido, P. Harris, L. Burns, L. Renteria, J. Woods, L. Chen, J. Allard, P. Ravindran, H. Bitter, Z. Liang, C. M. Hogaboam, C. Kitson, D. C. Budd, J. S. Fine, C. MT. Bauer, C. S. Stevenson, Bleomycin Induces Molecular Changes Directly Relevant to Idiopathic Pulmonary Fibrosis: A Model for "Active" Disease. *PLoS One*. **8**, e59348 (2013).

39. A. Laurence, C. M. Tato, T. S. Davidson, Y. Kanno, Z. Chen, Z. Yao, R. B. Blank, F. Meylan, R. Siegel, L. Hennighausen, E. M. Shevach, J. J. O'shea, Interleukin-2 signaling via STAT5 constrains T helper 17 cell generation. *Immunity*. **26**, 371–81 (2007).

40. Y. Ishida, T. Kondo, T. Takayasu, Y. Iwakura, N. Mukaida, The essential involvement of cross-talk between IFN-gamma and TGF-beta in the skin wound-healing process. *J Immunol*. **172**, 1848–55 (2004).

41. I.-K. Park, J. J. Letterio, J. D. Gorham, TGF-beta 1 inhibition of IFN-gamma-induced signaling and Th1 gene expression in CD4+ T cells is Smad3 independent but MAP kinase dependent. *Mol Immunol*. **44**, 3283–90 (2007).

42. A. V Misharin, L. Morales-Nebreda, P. A. Reyfman, C. M. Cuda, J. M. Walter, A. C. McQuattie-Pimentel, C.-I. Chen, K. R. Anekalla, N. Joshi, K. J. N. Williams, H. Abdala-Valencia, T. J. Yacoub, M. Chi, S. Chiu, F. J. Gonzalez-Gonzalez, K. Gates, A. P. Lam, T. T.

Nicholson, P. J. Homan, S. Soberanes, S. Dominguez, V. K. Morgan, R. Saber, A. Shaffer, M. Hinchcliff, S. A. Marshall, A. Bharat, S. Berdnikovs, S. M. Bhorade, E. T. Bartom, R. I. Morimoto, W. E. Balch, J. I. Sznajder, N. S. Chandel, G. M. Mutlu, M. Jain, C. J. Gottardi, B. D. Singer, K. M. Ridge, N. Bagheri, A. Shilatifard, G. R. S. Budinger, H. Perlman, Monocyte-derived alveolar macrophages drive lung fibrosis and persist in the lung over the life span. *J Exp Med*. **214**, 2387–2404 (2017).

43. A. L. McCubbrey, L. Barthel, M. P. Mohning, E. F. Redente, K. J. Mould, S. M. Thomas, S. M. Leach, T. Danhorn, S. L. Gibbings, C. V Jakubzick, P. M. Henson, W. J. Janssen, Deletion of c-FLIP from CD11bhi Macrophages Prevents Development of Bleomycin-induced Lung Fibrosis. *Am J Respir Cell Mol Biol*. **58**, 66–78 (2018).

44. M. A. Gibbons, A. C. MacKinnon, P. Ramachandran, K. Dhaliwal, R. Duffin, A. T. Phythian-Adams, N. van Rooijen, C. Haslett, S. E. Howie, A. J. Simpson, N. Hirani, J. Gauldie, J. P. Iredale, T. Sethi, S. J. Forbes, Ly6Chi monocytes direct alternatively activated profibrotic macrophage regulation of lung fibrosis. *Am J Respir Crit Care Med*. **184**, 569–81 (2011).

45. M. Kreuter, J. S. Lee, A. Tzouvelekis, J. M. Oldham, P. L. Molyneaux, D. Weycker, M. Atwood, K.-U. Kirchgaessler, T. M. Maher, Monocyte Count as a Prognostic Biomarker in Patients with Idiopathic Pulmonary Fibrosis. *Am J Respir Crit Care Med*. **204**, 74–81 (2021).

46. M. K. D. Scott, K. Quinn, Q. Li, R. Carroll, H. Warsinske, F. Vallania, S. Chen, M. A. Carns, K. Aren, J. Sun, K. Koloms, J. Lee, J. Baral, J. Kropski, H. Zhao, E. Herzog, F. J. Martinez, B. B. Moore, M. Hinchcliff, J. Denny, N. Kaminski, J. D. Herazo-Maya, N. H. Shah, P. Khatri, Increased monocyte count as a cellular biomarker for poor outcomes in fibrotic diseases: a retrospective, multicentre cohort study. *Lancet Respir Med*. **7**, 497–508 (2019).

47. A. Achaiah, A. Rathnapala, A. Pereira, H. Bothwell, K. Dwivedi, R. Barker, R. Benamore, R. K. Hoyles, V. Iotchkova, L.-P. Ho, Monocyte and neutrophil levels are potentially linked to progression to IPF for patients with indeterminate UIP CT pattern. *BMJ Open Respir Res*. **8**, e000899 (2021).

48. Y.-Z. Liu, S. Saito, G. F. Morris, C. A. Miller, J. Li, J. J. Lefante, Proportions of resting memory T cells and monocytes in blood have prognostic significance in idiopathic pulmonary fibrosis. *Genomics*. **111**, 1343–1350 (2019).

49. Y. Morimoto, K. Hirahara, M. Kiuchi, T. Wada, T. Ichikawa, T. Kanno, M. Okano, K. Kokubo, A. Onodera, D. Sakurai, Y. Okamoto, T. Nakayama, Amphiregulin-Producing Pathogenic Memory T Helper 2 Cells Instruct Eosinophils to Secrete Osteopontin and Facilitate Airway Fibrosis. *Immunity*. **49**, 134-150.e6 (2018).

50. D. Ferrari, C. Pizzirani, E. Adinolfi, R. M. Lemoli, A. Curti, M. Idzko, E. Panther, F. Di Virgilio, The P2X $_7$ Receptor: A Key Player in IL-1 Processing and Release. *The Journal of Immunology*. **176**, 3877–3883 (2006).

51. R. G. Jenkins, B. B. Moore, R. C. Chambers, O. Eickelberg, M. Königshoff, M. Kolb, G. J. Laurent, C. B. Nanthakumar, M. A. Olman, A. Pardo, M. Selman, D. Sheppard, P. J. Sime, A. M. Tager, A. L. Tatler, V. J. Thannickal, E. S. White, An Official American Thoracic Society Workshop Report: Use of Animal Models for the Preclinical Assessment of Potential Therapies for Pulmonary Fibrosis. *Am J Respir Cell Mol Biol*. **56**, 667–679 (2017).

52. N. Khalil, R. N. O'Connor, H. W. Unruh, P. W. Warren, K. C. Flanders, A. Kemp, O. H. Bereznay, A. H. Greenberg, Increased production and immunohistochemical localization of transforming growth factor-beta in idiopathic pulmonary fibrosis. *Am J Respir Cell Mol Biol*. **5**, 155–62 (1991).

53. A. Koutoulaki, M. Langley, A. J. Sloan, D. Aeschlimann, X.-Q. Wei, TNFalpha and TGF-beta1 influence IL-18-induced IFNgamma production through regulation of IL-18 receptor and T-bet expression. *Cytokine*. **49**, 177–84 (2010).

54. F. Di Virgilio, M. Vuerich, Purinergic signaling in the immune system. *Auton Neurosci*. **191**, 117–23 (2015).

55. P. J. Sáez, P. Vargas, K. F. Shoji, P. A. Harcha, A.-M. Lennon-Duménil, J. C. Sáez, ATP promotes the fast migration of dendritic cells through the activity of pannexin 1 channels and P2X7 receptors. *Sci Signal*. **10** (2017), doi:10.1126/scisignal.aah7107.

56. Y. Iwai, H. Hemmi, O. Mizenina, S. Kuroda, K. Suda, R. M. Steinman, An IFN-gamma-IL-18 signaling loop accelerates memory CD8+ T cell proliferation. *PLoS One*. **3**, e2404 (2008).

57. G. Penton-Rol, N. Polentarutti, W. Luini, A. Borsatti, R. Mancinelli, A. Sica, S. Sozzani, A. Mantovani, Selective inhibition of expression of the chemokine receptor CCR2 in human monocytes by IFN-gamma. *J Immunol*. **160**, 3869–73 (1998).

58. A. M. de Bruin, M. Buitenhuis, K. F. van der Sluijs, K. P. J. M. van Gisbergen, L. Boon, M. A. Nolte, Eosinophil differentiation in the bone marrow is inhibited by T cell-derived IFN-gamma. *Blood*. **116**, 2559–69 (2010).

59. I. Iwamoto, H. Nakajima, H. Endo, S. Yoshida, Interferon gamma regulates antigen-induced eosinophil recruitment into the mouse airways by inhibiting the infiltration of CD4+ T cells. *J Exp Med*. **177**, 573–6 (1993).

60. G. Raghu, B. Rochwerg, Y. Zhang, C. A. C. Garcia, A. Azuma, J. Behr, J. L. Brozek, H. R. Collard, W. Cunningham, S. Homma, T. Johkoh, F. J. Martinez, J. Myers, S. L. Protzko, L. Richeldi, D. Rind, M. Selman, A. Theodore, A. U. Wells, H. Hoogsteden, H. J. Schünemann, American Thoracic Society, European Respiratory society, Japanese Respiratory Society, Latin American Thoracic Association, An Official ATS/ERS/JRS/ALAT

Clinical Practice Guideline: Treatment of Idiopathic Pulmonary Fibrosis. An Update of the 2011 Clinical Practice Guideline. *Am J Respir Crit Care Med*. **192**, e3-19 (2015).

61. I. Lasithiotaki, E. Tsitoura, K. D. Samara, A. Trachalaki, I. Charalambous, N. Tzanakis, K. M. Antoniou, NLRP3/Caspase-1 inflammasome activation is decreased in alveolar macrophages in patients with lung cancer. *PLoS One*. **13**, e0205242 (2018).

62. I. Lasithiotaki, I. Giannarakis, E. Tsitoura, K. D. Samara, G. A. Margaritopoulos, C. Choulaki, E. Vasarmidi, N. Tzanakis, A. Voloudaki, P. Sidiropoulos, N. M. Siafakas, K. M. Antoniou, NLRP3 inflammasome expression in idiopathic pulmonary fibrosis and rheumatoid lung. *Eur Respir J*. **47**, 910–8 (2016).

63. A. S. Patel, L. Lin, A. Geyer, J. A. Haspel, C. H. An, J. Cao, I. O. Rosas, D. Morse, Autophagy in idiopathic pulmonary fibrosis. *PLoS One*. **7**, e41394 (2012).

64. C. N. J. Young, A. Sinadinos, A. Lefebvre, P. Chan, S. Arkle, D. Vaudry, D. C. Gorecki, A novel mechanism of autophagic cell death in dystrophic muscle regulated by P2RX7 receptor large-pore formation and HSP90. *Autophagy*. **11**, 113–30 (2015).

65. N. Dupont, S. Jiang, M. Pilli, W. Ornatowski, D. Bhattacharya, V. Deretic, Autophagy-based unconventional secretory pathway for extracellular delivery of IL-1β. *EMBO J*. **30**, 4701–11 (2011).

66. C. M. Artlett, S. Sassi-Gaha, J. L. Rieger, A. C. Boesteanu, C. A. Feghali-Bostwick, P. D. Katsikis, The inflammasome activating caspase 1 mediates fibrosis and myofibroblast differentiation in systemic sclerosis. *Arthritis Rheum*. **63**, 3563–74 (2011).

67. L. A. Cameron, R. A. Taha, A. Tsicopoulos, M. Kurimoto, R. Olivenstein, B. Wallaert, E. M. Minshall, Q. A. Hamid, Airway epithelium expresses interleukin-18. *Eur Respir J*. **14**, 553–9 (1999).

68. A. Watanabe, M. A. Sohail, D. A. Gomes, A. Hashmi, J. Nagata, F. S. Sutterwala, S. Mahmood, M. N. Jhandier, Y. Shi, R. A. Flavell, W. Z. Mehal, Inflammasome-mediated

regulation of hepatic stellate cells. *Am J Physiol Gastrointest Liver Physiol*. **296**, G1248-57 (2009).

69. A. A. Pinar, A. Yuferov, T. A. Gaspari, C. S. Samuel, Relaxin Can Mediate Its Anti-Fibrotic Effects by Targeting the Myofibroblast NLRP3 Inflammasome at the Level of Caspase-1. *Front Pharmacol*. **11**, 1201 (2020).

70. M. H. Sharawy, M. S. Serrya, Pirfenidone attenuates gentamicin-induced acute kidney injury by inhibiting inflammasome-dependent NLRP3 pathway in rats. *Life Sci*. **260**, 118454 (2020).

71. H. Oku, T. Shimizu, T. Kawabata, M. Nagira, I. Hikita, A. Ueyama, S. Matsushima, M. Torii, A. Arimura, Antifibrotic action of pirfenidone and prednisolone: different effects on pulmonary cytokines and growth factors in bleomycin-induced murine pulmonary fibrosis. *Eur J Pharmacol*. **590**, 400–8 (2008).

72. E. Mavrogiannis, Q. A. J. Hagdorn, V. Bazioti, J. M. Douwes, D. E. Van Der Feen, S. U. Oberdorf-Maass, M. Westerterp, R. M. F. Berger, Pirfenidone ameliorates pulmonary arterial pressure and neointimal remodeling in experimental pulmonary arterial hypertension by suppressing NLRP3 inflammasome activation. *Pulm Circ*. **12**, e12101 (2022).

73. P. Spagnolo, J. A. Kropski, M. G. Jones, J. S. Lee, G. Rossi, T. Karampitsakos, T. M. Maher, A. Tzouvelekis, C. J. Ryerson, Idiopathic pulmonary fibrosis: Disease mechanisms and drug development. *Pharmacol Ther*. **222**, 107798 (2021).

74. R.-H. Hübner, W. Gitter, N. Eddine El Mokhtari, M. Mathiak, M. Both, H. Bolte, S. Freitag-Wolf, B. Bewig, Standardized quantification of pulmonary fibrosis in histological samples. *Biotechniques*. **44**, 507–517 (2008).

75. J. Schindelin, I. Arganda-Carreras, E. Frise, V. Kaynig, M. Longair, T. Pietzsch, S. Preibisch, C. Rueden, S. Saalfeld, B. Schmid, J.-Y. Tinevez, D. J. White, V. Hartenstein, K.

Eliceiri, P. Tomancak, A. Cardona, Fiji: an open-source platform for biological-image analysis. *Nat Methods*. **9**, 676–682 (2012).

Figure legends

Figure 1. The P2RX7/IL-18/IFN-γ pathway is downregulated in IPF

(A) Heatmap of mRNA expression of P2RX7 in control and IPF patients with a cluster of fibrosis-associated genes. Raw p-values are shown (Limma). (B) mRNA expression of *P2RX7, IL18, IL18R1, IL18RAP* and *IFNG* between control and IPF patients from 213 individuals, corresponding to 91 controls and 122 IPF patients. Two-tailed unpaired t-test with Welch's correction, ***$p < 0.001$, ****$p < 0.0001$. (C) Gene set enrichment analysis (GSEA) plot associating P2RX7 mRNA levels from IPF patients with three immunological signatures. The green line represents the enrichment score and the black lines the specific signature-associated genes. NES: Normalized enrichment score, FDR: False discovery rate. Pearson's correlation test.

Figure 2. Activation of P2RX7 with HEI3090 inhibits lung fibrosis progression

(A) Experimental design. WT mice were given 2.5 U/kg of bleomycin by i.n. route. At the end of the inflammatory phase, 1.5 mg/kg of HEI3090 or vehicle were given daily until day 21. (B) Representative images of lung sections at day 21 after treatment stained with H&E and Sirius Red, Scale bar= 100 µm. (C) Fibrosis score assessed by the Ashcroft method. (D) Collagen levels in whole lung of mice assessed on Sirius Red-polarized images. (E) Experimental design. WT mice were given 2.5 U/kg of bleomycin by i.n. route. 1.5 mg/kg of HEI3090 or vehicle were given daily until day 14. (F) Representative images of lung sections at day 14 after treatment stained with H&E and Sirius Red, Scale bar= 100 µm. (G) Fibrosis score assessed by the Ashcroft method. (H) Collagen levels in whole lung of mice assessed on Sirius Red-polarized images. Each point represents one mouse, two-tailed Mann-Whitney test, p values: *$p < 0.05$, **$p < 0.01$. WT: Wildtype, BLM: bleomycin, i.p.: intraperitoneal, i.n.: intranasal, H&E: hematoxylin & eosin, AU: arbitrary units.

Figure 3. HEI3090 favors an anti-fibrotic immune signature in the lungs

(A) WT mice were given 2.5 U/kg of bleomycin by i.n. route and treated daily i.p. with 1.5 mg/kg of HEI3090 or Vehicle. Lungs were analyzed by flow cytometry at day 14. (A) Contour plot of IFN-γ and IL-17A producing T cells ($CD3^+NK1.1^-$) (left) and ratio of IFN-γ over IL-17A in T cells ($CD3^+NK1.1^-$) (right). (B) Percentage of IFN-γ producing $CD4^+$ and $CD8^+$ T cells. (C) Percentage and GMFI of IL-$17A^+$ cells of $CD4^+$ T cells ($CD3^+CD4^+NK1.1^-$). (D) Percentage and GMFI of TGFβ in $CD45^+$ cells. (E) Dotplot showing lung inflammatory monocytes, gated on $lineage^-CD11c^-CD11b^+$ cells (left) and percentage of lung inflammatory monocytes ($Ly6C^{high}Ly6G^-$) (right) (F) Percentage of alveolar macrophages ($CD11c^+SiglecF^+$) and (G) lung eosinophils ($CD11b^+SiglecF^+CD11c^-$). Each point represents one mouse, data represented as violin plots or mean±SEM, two-tailed Mann-Whitney test, *$p < 0.05$, **$p < 0.01$. GMFI: geometric mean fluorescence intensity. i.n.: intranasal, i.p.: intraperitoneal.

Figure 4. The P2RX7/NLRP3/IL-18 pathway in immune cells is required for HEI3090's antifibrotic effect

(A) Experimental design. p2rx7-/- mice were given 3.106 WT, nlrp3-/- or il18-/- splenocytes i.v. one day prior to BLM delivery (i.n. 2.5 U/kg). Mice were treated daily i.p. with 1.5 mg/kg HEI3090 or vehicle for 14 days. (B,D,F) Representative images of lung sections at day 14 after treatment stained with H&E and Sirius Red, scale bar= 100 µm. Fibrosis score assessed by the Ashcroft method of adoptive transfer of WT splenocytes, (E) nlrp3-/- splenocytes and (G) il18-/- splenocytes. (H) IL-18 levels in sera of WT BLM-induced mice at day 14 (I) Ratio of IFN-γ over IL-17A in lung T cells (CD3+NK1.1-) of WT mice neutralized for IL-18 or not (isotype control) every 3 days. Each point represents one mouse, two-tailed Mann-Whitney test, *$p < 0.05$. WT: Wildtype, BLM: bleomycin, i.p.: intraperitoneal, i.n.: intranasal, i.v.: intravenous, H&E: hematoxylin & eosin.

Table 1. Antibodies used in this study

Antibody	Dilution	Fluorochrome	Clone	Reference	Supplier
CD16/CD32	1/100		2.4G2	553142	BD Biosciences
CD3ε	1/100	PerCP-Cy5.5	145-2611	551163	
NK1.1	1/100	PE-CF594	PK136	562864	
CD11c	1/100	PE-Cy7	HL3	558079	
Ly6G	1/100	AF700	1A8	561236	
Ly6C	1/100	V450	AL-21	560594	
SiglecF	1/50	BV605	E50-2440	740388	
CD4	1/100	BV711	RM4-5	563726	
CD8α	1/100	BV650	53-6.7	100741	
CD45.2	1/100	BV786	104	563686	
CD45	1/100	BUV395	30-F11	564279	
γδ TCR	1/100	PE	GL3	553178	
IFNγ	1/100	APC	XMG1.2	554413	
IL-17A	1/100	AF700	TC11-18H10	561718	
I-A/I-E	1/100	APCfire750	M5/114.15.2	107651	Biolegend
CD64	1/20	PE	X54-5/7.1	139303	
P2RX7	1/8	PE	1F11	148706	
CD11b	1/400	APC	M1/70	17-0112-82	eBiosciences
Foxp3	1/100	PE	FJK16S	12-5773-82	
NLRP3	1/1000		Cryo-2	AG-20B-0014	Adipogen
ACTIN BETA	1/60000		monoclonal	VMA00048	Biorad
IL-18	1/250		polyclonal	5180R-100	Biovision
IL-18	200 µg		YIGIF74-1G7	BE0237	BioXcell
Isotype Control Rat IgG2a, κ	200 µg		2A3	BE0089	BioXcell

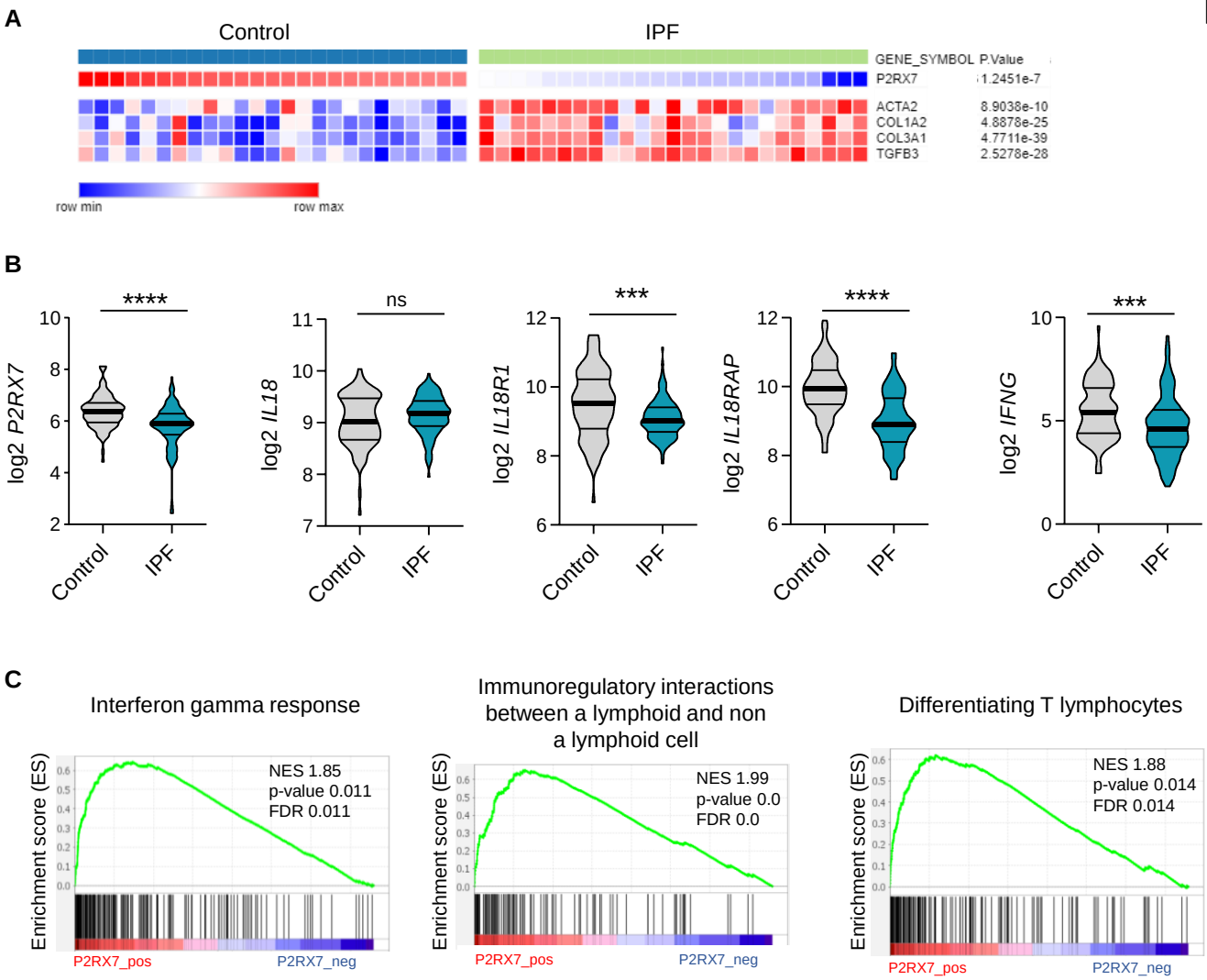

Figure 1 : The P2RX7/IL-18/IFN-γ pathway is downregulated in IPF

(A) Heatmap of mRNA expression of P2RX7 in control and IPF patients with a cluster of fibrosis-associated genes. Raw p-values are shown (Limma). **(B)** mRNA expression of *P2RX7, IL18, IL18R1, IL18RAP* and *IFNG* between control and IPF patients. 213 individuals, corresponding to 91 controls and 122 IPF patients. Two-tailed unpaired t-test with Welch's correction, ***$p < 0.001$, ****$p < 0.0001$. **(C)** Gene set enrichment analysis (GSEA) plot associating P2RX7 mRNA levels from IPF patients with three immunological signatures. The green line represents the enrichment score and the black lines the specific signature-associated genes. NES: Normalized enrichment score, FDR: False discovery rate. Pearson's correlation test.

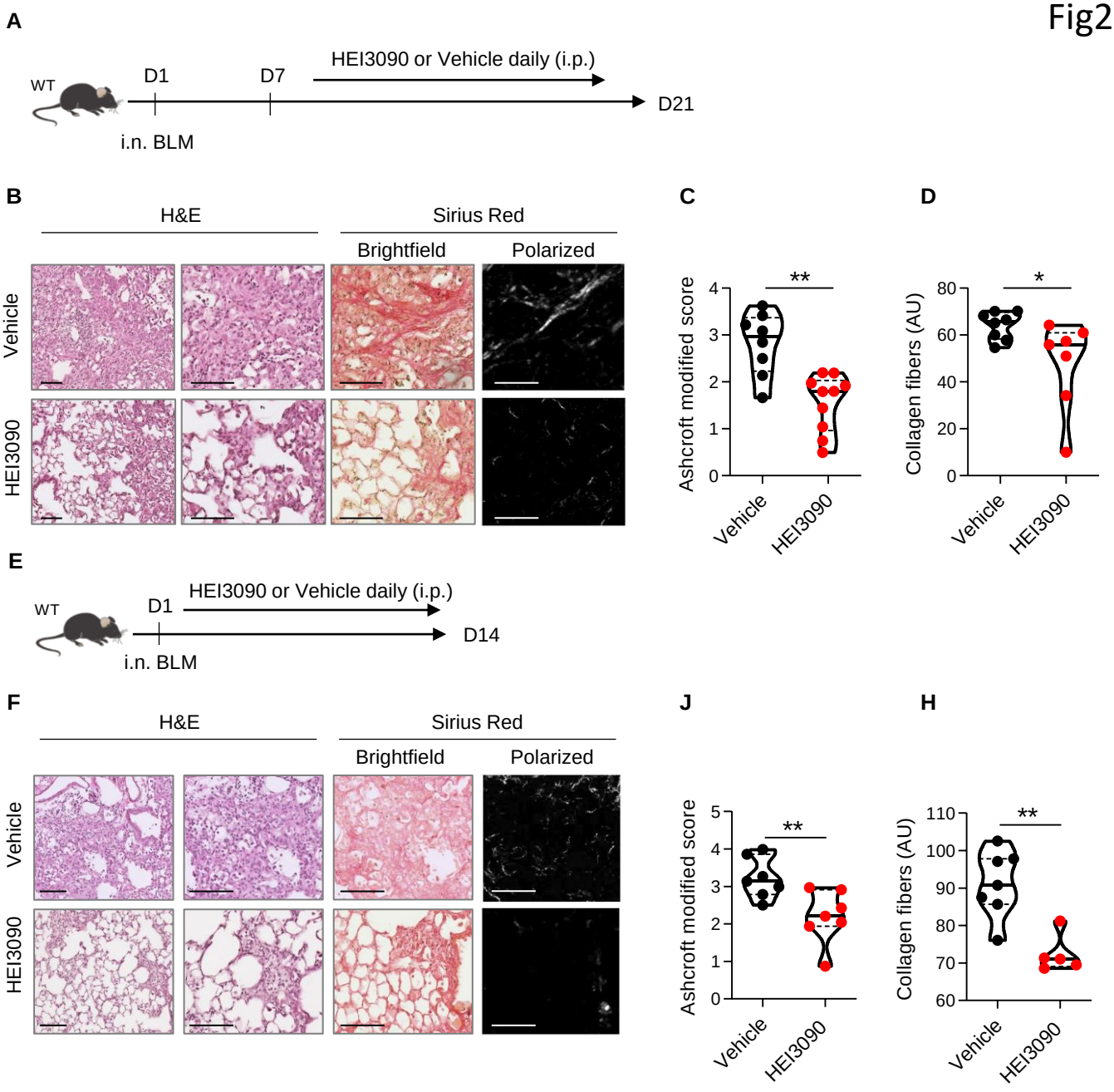

Figure 2 : Activation of P2RX7 with HEI3090 inhibits lung fibrosis progression

(A) Experimental design. WT mice were given 2.5 U/kg of bleomycin by i.n. route. At the end of the inflammatory phase, 1.5 mg/kg of HEI3090 or vehicle were given daily until day 21. **(B)** Representative images of lung sections at day 21 after treatment stained with H&E and Sirius Red, Scale bar= 100 µm. **(C)** Fibrosis score assessed by the Ashcroft method. **(D)** Collagen levels in whole lung of mice assessed on Sirius Red-polarized images. **(E)** Experimental design. WT mice were given 2.5 U/kg of bleomycin by i.n. route. 1.5 mg/kg of HEI3090 or vehicle were given daily until day 14. **(F)** Representative images of lung sections at day 14 after treatment stained with H&E and Sirius Red, Scale bar= 100 µm. **(G)** Fibrosis score assessed by the Ashcroft method. **(H)** Collagen levels in whole lung of mice assessed on Sirius Red-polarized images. Each point represents one mouse, two-tailed Mann-Whitney test, p values: *$p < 0.05$, **$p < 0.01$. WT: Wildtype, BLM: bleomycin, i.p.: intraperitoneal, i.n.: intranasal, H&E: hematoxylin&eosin, AU: arbitrary units

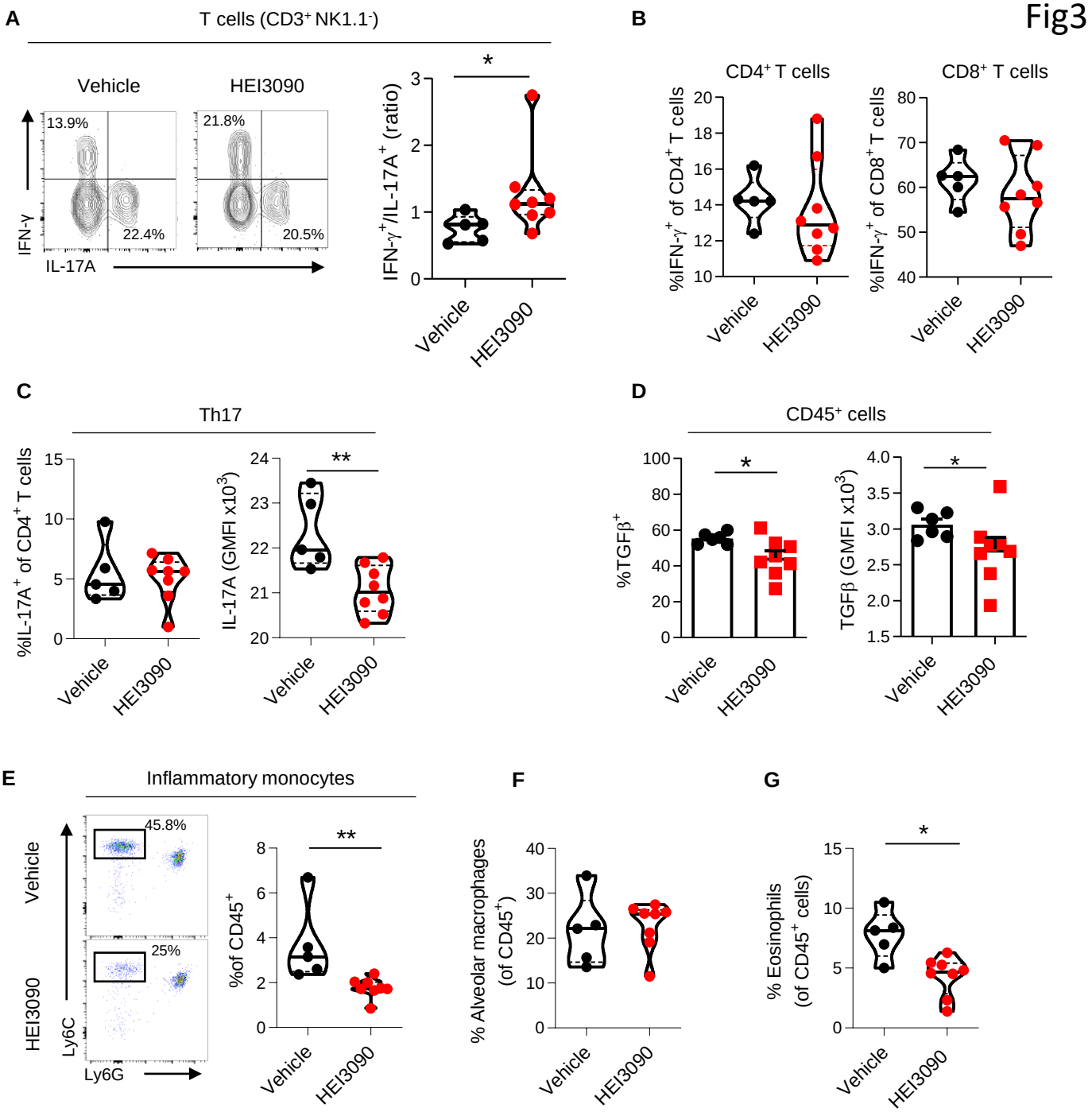

Figure 3 : HEI3090 favors an anti-fibrotic immune signature in the lungs

WT mice were given 2.5 U/kg of bleomycin by i.n. route and treated daily i.p. with 1.5 mg/kg of HEI3090 or Vehicle. Lungs were analyzed by flow cytometry at day 14. **(A)** Contour plot of IFN-γ and IL-17A producing T cells ($CD3^+NK1.1^-$) (left) and ratio of IFN-γ over IL-17A in T cells ($CD3^+NK1.1^-$) (right). **(B)** Percentage of IFN-γ producing $CD4^+$ and $CD8^+$ T cells. **(C)** Percentage and GMFI of IL-17A$^+$ cells of $CD4^+$ T cells ($CD3^+CD4^+NK1.1^-$). **(D)** Percentage and GMFI of TGFβ in $CD45^+$ cells. **(E)** Dotplot showing lung inflammatory monocytes, gated on lineage$^-$CD11c$^-$CD11b$^+$ cells (left) and percentage of lung inflammatory monocytes (Ly6C^{high}Ly6G$^-$) (right) **(F)** Percentage of alveolar macrophages ($CD11c^+SiglecF^+$) and **(G)** lung eosinophils ($CD11b^+SiglecF^+CD11c^-$). Each point represents one mouse, data represented as violin plots or mean±SEM, two-tailed Mann-Whitney test, *p < 0.05, **p < 0.01. GMFI: geometric mean fluorescence intensity. i.n.: intranasal, i.p.: intraperitoneal

Fig4

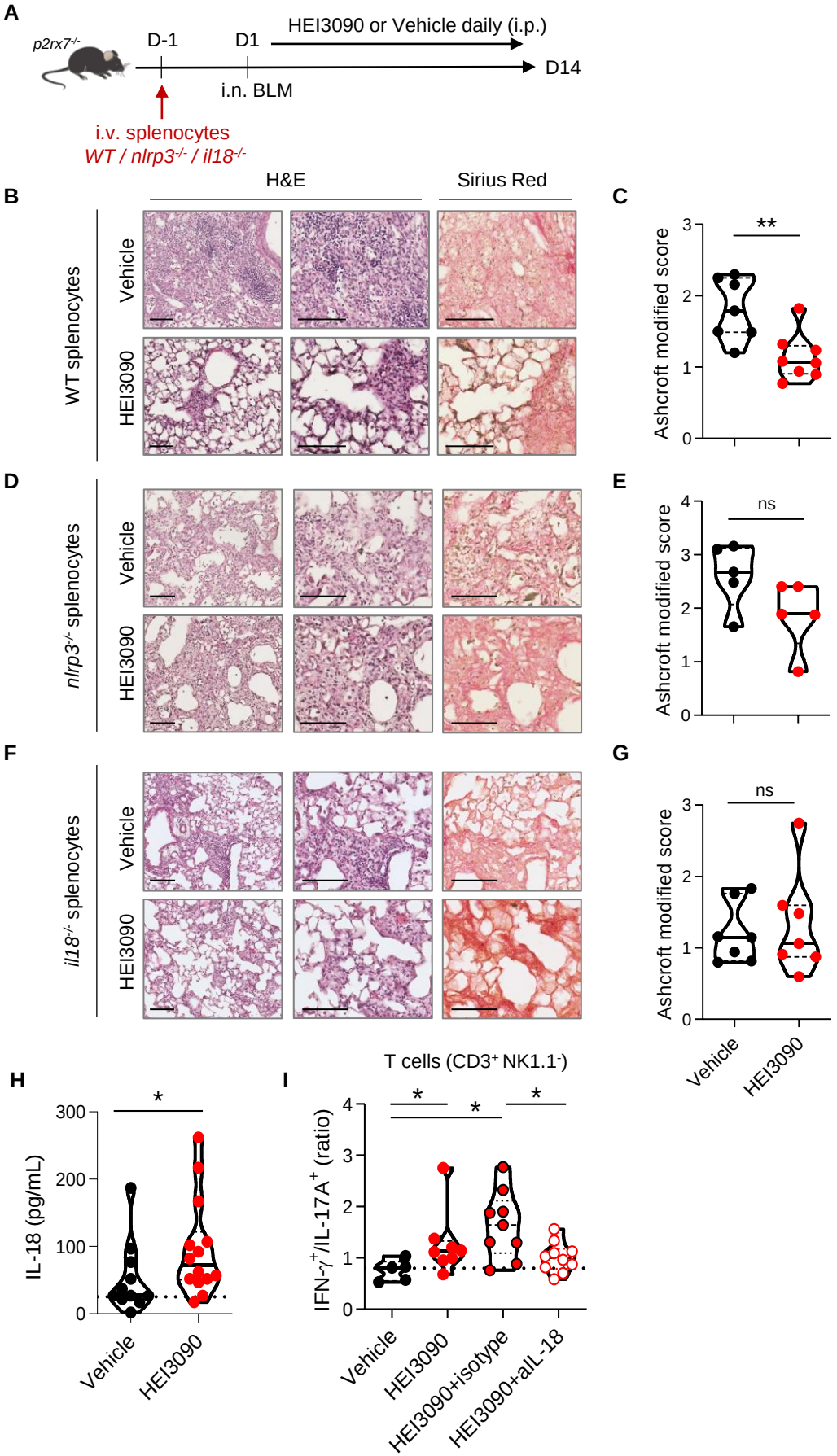

Figure 4: The P2RX7/NLRP3/IL-18 pathway in immune cells is required for HEI3090's antifibrotic effect

(A) Experimental design. *p2rx7*$^{-/-}$ mice were given 3.10^6 WT, *nlrp3*$^{-/-}$ or *il18*$^{-/-}$ splenocytes i.v. one day prior to BLM delivery (i.n. 2.5 U/kg). Mice were treated daily i.p. with 1.5 mg/kg HEI3090 or vehicle for 14 days. **(B,D,F)** Representative images of lung sections at day 14 after treatment stained with H&E and Sirius Red, scale bar= 100 µm. Fibrosis score assessed by the Ashcroft method of adoptive transfer of WT splenocytes, **(E)** *nlrp3*$^{-/-}$ splenocytes and **(G)** *il18*$^{-/-}$ splenocytes. **(H)** IL-18 levels in sera of WT BLM-induced mice at day 14 **(I)** Ratio of IFN-γ over IL-17A in lung T cells ($CD3^+NK1.1^-$) of WT mice neutralized for IL-18 or not (isotype control) every 3 days. Each point represents one mouse, two-tailed Mann-Whitney test, *$p < 0.05$. WT: Wildtype, BLM: bleomycin, i.p.: intraperitoneal, i.n.: intranasal, i.v.: intravenous, H&E: hematoxylin&eosin